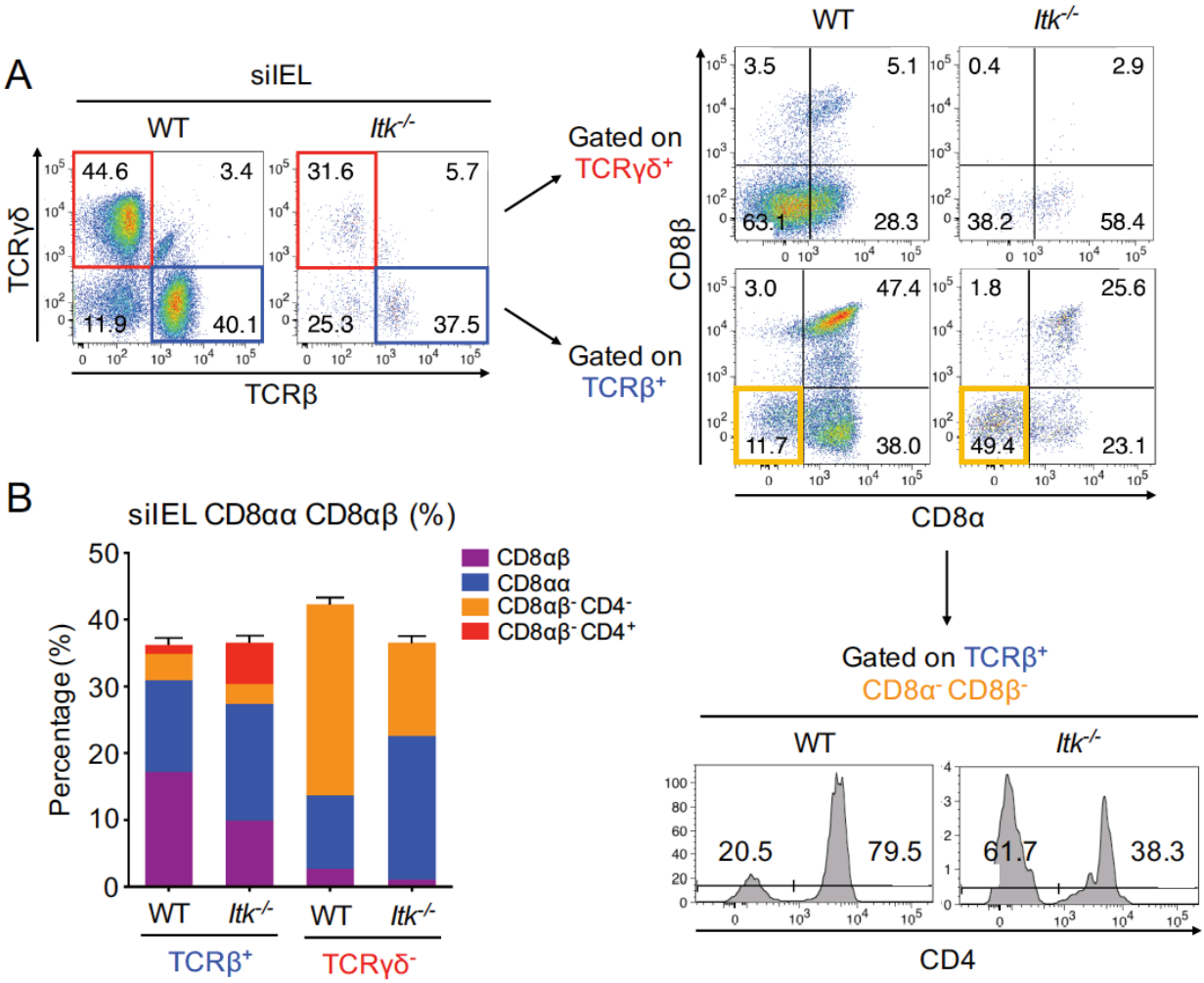

Supplemental Fig. 1. Similar subset composition of gut-resident TCRβ$^+$ and TCRγδ$^+$ IELs in the small intestines of WT and *Itk*$^{-/-}$ mice

(A-B) Flow cytometric analysis of intraepithelial lymphocytes from small intestines (siIEL) of naïve WT and *Itk*$^{-/-}$ mice. Cells shown are gated on lymphocytes (top row). Gated TCRβ$^+$ (blue box, left two plots) or TCRγδ$^+$ (red box, right two plots) cells were examined for CD8αα versus CD8αβ staining (middle row). Gated TCRβ$^+$ CD8α$^-$ CD8β$^-$ cells were examined for CD4 expression (bottom row) (A). Compilation of data from 4-7 mice per genotype indicate the relative proportions of each subset (B).

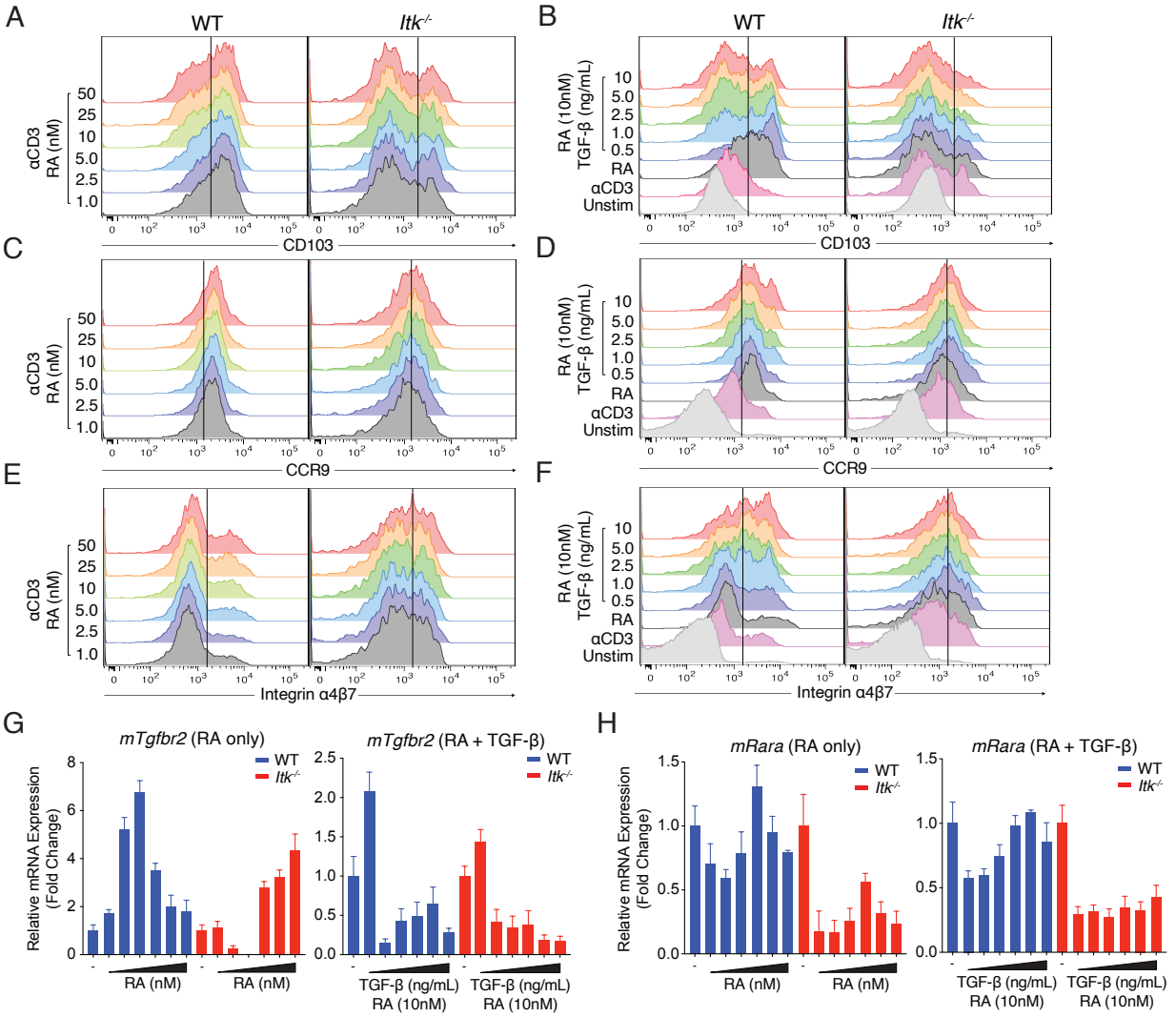

Supplemental Fig. 2. Titrations of RA and TGF-β reveal the global unresponsiveness of *Itk*$^{-/-}$ CD8^{+} T cells to these factors

(A-F) Isolated WT and *Itk*$^{-/-}$ OT-I CD8^{+} T cells were stimulated with anti-CD3 (1.0 μg/mL) in the presence or absence of TGF-β (0.5 to 10 ng/mL) plus RA (10nM or 1.0 to 50nM) for 48 h, and CD103 (A-B), CCR9 (C-D), and integrin α4β7 (E-F) expression were examined. (G-H) mRNA expression of *Tgfbr2* (G) and *Rara* (H) from the same experiments are shown. Data are compiled from 2-3 independent experiments.

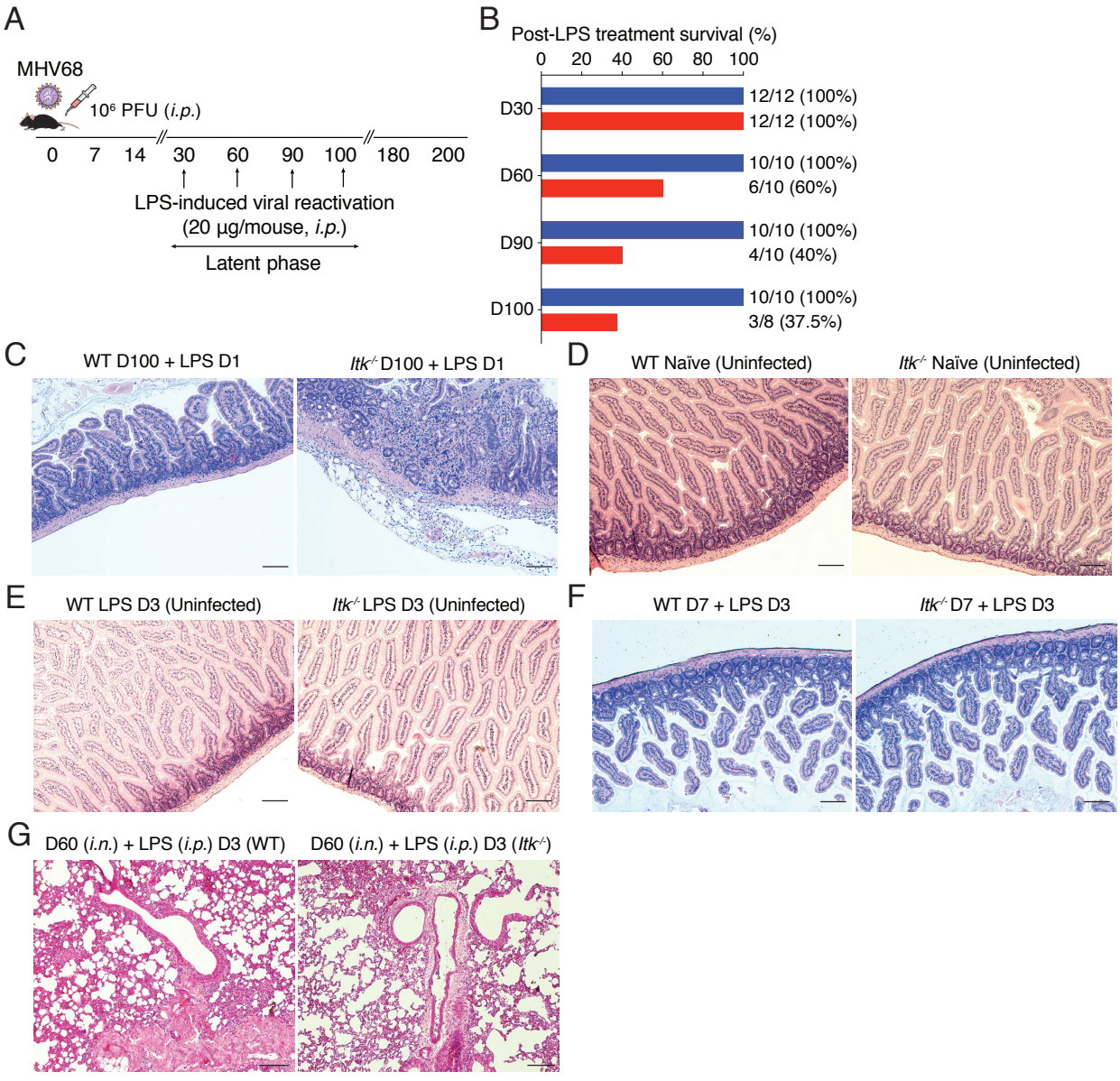

Supplemental Fig. 3. Lethal inflammation in the gut, but not the lung, of *Itk*$^{-/-}$ mice is induced by LPS administration to MHV68 latently-infected but not uninfected mice

(A) A single dose of LPS (20 µg) was injected (*i.p.*) into MHV68-infected (*i.p.*) WT and *Itk*$^{-/-}$ hosts at varying timepoints during latency. (B) Percentage survival of WT and *Itk*$^{-/-}$ infected mice after LPS injection. (C-F) Histologic analyses of duodenum from LPS-treated (D1) MHV68-infected (D100) (C), uninfected naïve (D), LPS-treated (D3) uninfected (E), and LPS-treated (D3) MHV68-infected (D7) (F) WT and *Itk*$^{-/-}$ mice. (G) Histology of lungs from MHV68-infected mice (*i.n.*) at D60 after D3 of post-LPS injection (*i.p.*). Shown images are at 10X magnification. Bar, 75 µm. Data are representative of 4 mice of each genotype.

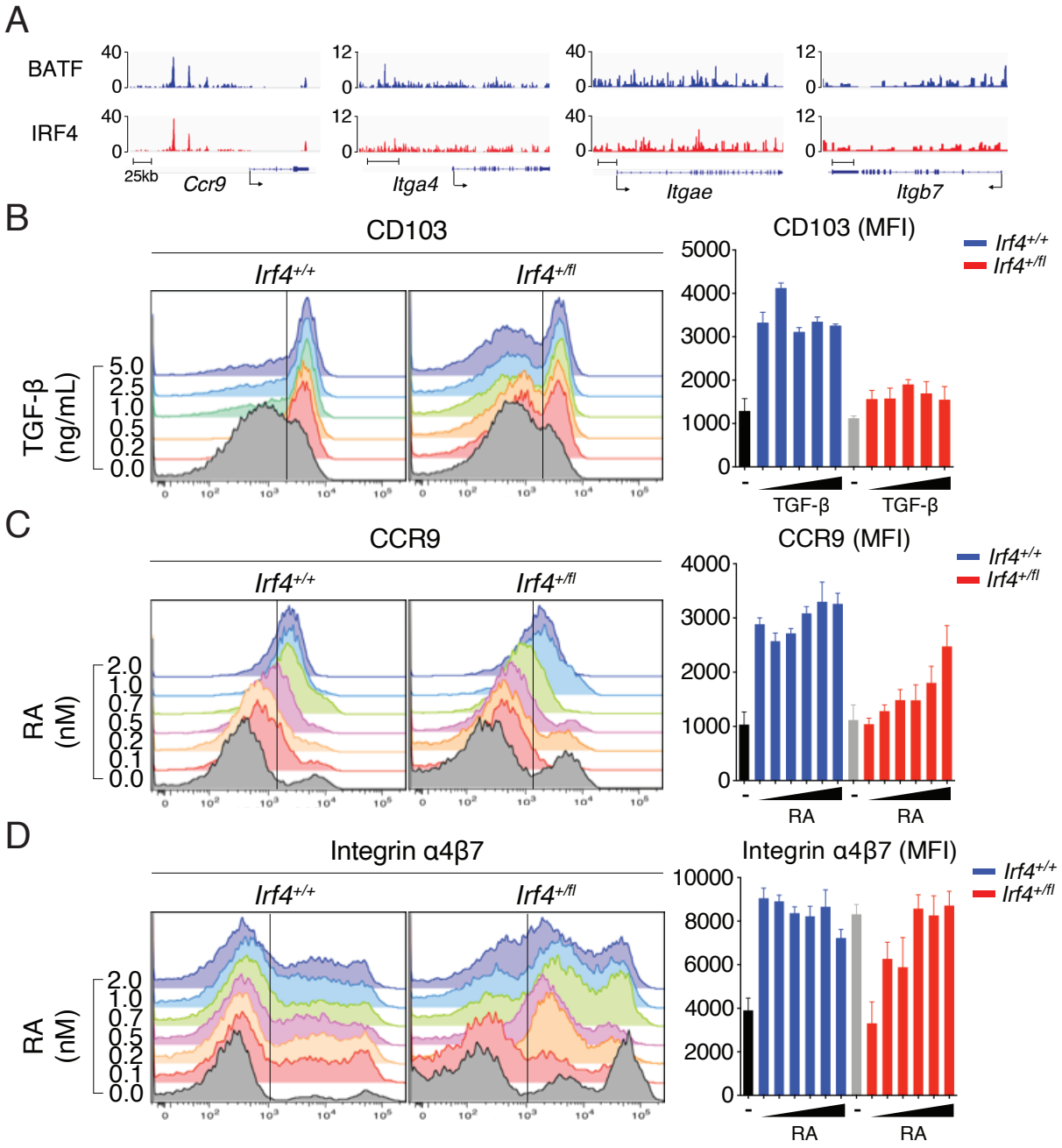

Supplemental Fig. 4. Correlation between IRF4 and the regulation of gut-homing receptor expression in CD8$^+$ T cells

(A) ChIP-Seq analysis of the binding of BATF and IRF4 to genomic regions in the proximity of *Ccr9*, *Itgae*, *Itga4*, and *Itgae* from NCBI GEO Database. (B-D) Spleen *Irf4*$^{+/+}$ and *Irf4*$^{+/fl}$ CD8$^+$ T cells were stimulated with anti-CD3 ± varying concentrations of TGF-β (0.2 to 5.0 ng/mL) or RA (0.1 to 2.0 nM) for 48 h, and CD103 (B), CCR9 (C), and integrin α4β7 (D) expression were analyzed. Mean fluorescence of each molecule was enumerated in the graph at the right.